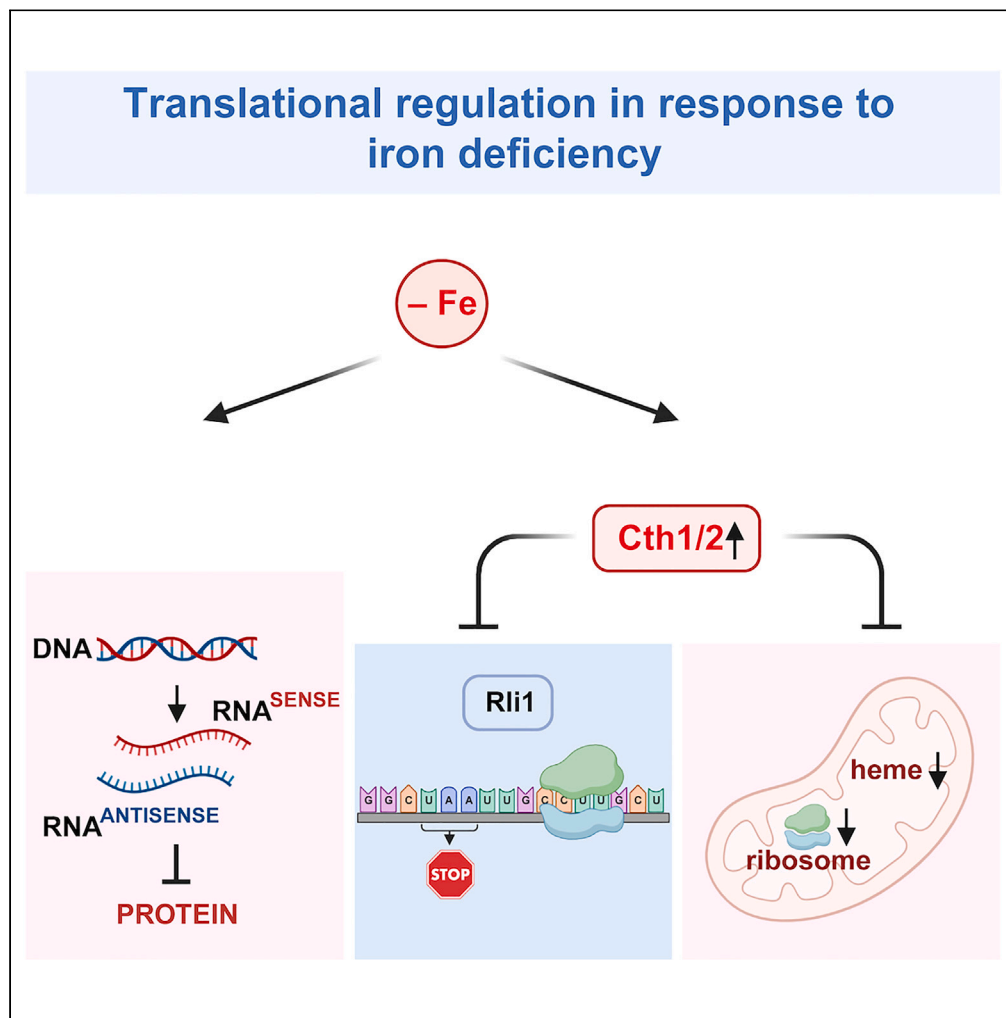


Article

Ribosome profiling reveals the role of yeast RNA-binding proteins Cth1 and Cth2 in translational regulation



Hanna Barlit,
Antonia M.
Romero, Ali
Gülhan, ..., Vadim
N. Gladyshev,
Sergi Puig,
Vyacheslav M.
Labunskyy

vlabuns@bu.edu

Highlights

Iron depletion represses translation of genes involved in iron-related processes

Cth1/2 mRNA-binding proteins inhibit mitochondrial translation and heme synthesis

Low iron increases translation in 3'UTRs due to Cth1/2-dependent inhibition of Rli1

MRS3 translation is repressed by low iron through expression of antisense lncRNA

Barlit et al., iScience 27, 109868
June 21, 2024 © 2024 The
Authors. Published by Elsevier
Inc.
<https://doi.org/10.1016/j.isci.2024.109868>



Article

Ribosome profiling reveals the role of yeast RNA-binding proteins Cth1 and Cth2 in translational regulation

Hanna Barlit,¹ Antonia M. Romero,² Ali Gülhan,¹ Praveen K. Patnaik,¹ Alexander Tyshkovskiy,³ María T. Martínez-Pastor,^{2,4} Vadim N. Gladyshev,³ Sergi Puig,² and Vyacheslav M. Labunsky^{1,5,*}

SUMMARY

Iron serves as a cofactor for enzymes involved in several steps of protein translation, but the control of translation during iron limitation is not understood at the molecular level. Here, we report a genome-wide analysis of protein translation in response to iron deficiency in yeast using ribosome profiling. We show that iron depletion affects global protein synthesis and leads to translational repression of multiple genes involved in iron-related processes. Furthermore, we demonstrate that the RNA-binding proteins Cth1 and Cth2 play a central role in this translational regulation by repressing the activity of the iron-dependent Rli1 ribosome recycling factor and inhibiting mitochondrial translation and heme biosynthesis. Additionally, we found that iron deficiency represses *MRS3* mRNA translation through increased expression of antisense long non-coding RNA. Together, our results reveal complex gene expression and protein synthesis remodeling in response to low iron, demonstrating how this important metal affects protein translation at multiple levels.

INTRODUCTION

Iron (Fe) is an essential trace element that serves as a cofactor for enzymes involved in numerous cellular processes, including protein translation, DNA replication and repair, lipid biosynthesis, and mitochondrial oxidative phosphorylation.¹ Dysregulation of Fe homeostasis has been implicated in health and disease. In humans, Fe deficiency causes anemia and leads to the decline of immune, neuronal, and muscle functions.^{2,3} On the other hand, Fe overload leads to organ failure, due to Fe toxicity, and the development of several disorders, such as Alzheimer's disease, cancer, and delayed wound healing.⁴ Moreover, imbalance in Fe metabolism has been implicated in aging and age-associated organ failure, but the exact mechanisms remain unclear.⁵ A better understanding of the mechanisms by which cells adapt to changes in Fe availability is required for the development of targeted therapeutic strategies against diseases associated with the dysregulation of Fe homeostasis.

Yeast *Saccharomyces cerevisiae* has proven to be a useful model for understanding the basic mechanisms of adaptation of eukaryotic cells to Fe depletion. Previous studies in yeast have shown that Fe deficiency leads to significant changes in gene expression^{6–8}. These changes are mediated by the Aft1 and Aft2 transcription factors, which activate the transcription of ~35 genes known as the “Fe regulon”. Expression of these genes allows cellular adaptation to low Fe through several mechanisms: (i) increasing Fe uptake into the cell, (ii) mobilizing Fe from vacuolar stores, and (iii) recycling Fe by promoting heme degradation.^{6,9,10} In addition, cells adapt to Fe deficiency by dropping the utilization of Fe for non-essential metabolic pathways and shifting to Fe-independent metabolism through the increased expression of the mRNA-binding protein Cth2, which is under the control of the Aft1/2 transcription factors. Cth2 recognizes and binds to AU-rich sequences (5'-UAUUUU-3' and 5'-UUUUUU-3') in the 3' untranslated region (3'UTR) of several mRNAs coding for proteins containing Fe as a cofactor (including aconitase, succinate dehydrogenase, and components of the mitochondrial electron transport chain) and stimulate their degradation.⁷ A paralog of Cth2, named Cth1, is 46% identical to Cth2, recognizes similar consensus sequences, and can repress the expression of a partially overlapping set of target genes.^{7,11,12} Thus, Cth1 and Cth2 remodel Fe metabolism prioritizing Fe for proteins involved in essential processes such as DNA replication and repair.¹³

While transcriptional responses to Fe deficiency have been extensively characterized, little is known about the role of Fe in regulating protein translation. Previous reports have shown that Fe deficiency leads to a global inhibition of protein synthesis, which is dependent on the TORC1 and Gcn2/eIF2 α pathways.^{8,14} In addition, Fe serves as a cofactor for several enzymes participating in protein translation, including

¹Department of Dermatology, Boston University Chobanian & Avedisian School of Medicine, Boston, MA, USA

²Departamento de Biotecnología, Instituto de Agroquímica y Tecnología de Alimentos (IATA), Consejo Superior de Investigaciones Científicas (CSIC), Valencia, Spain

³Division of Genetics, Department of Medicine, Brigham and Women's Hospital, Harvard Medical School, Boston, MA, USA

⁴Departamento de Bioquímica y Biología Molecular, Universitat de València, Valencia, Spain

⁵Lead contact

*Correspondence: vlabun@bu.edu

<https://doi.org/10.1016/j.isci.2024.109868>



proteins involved in modifications of factors affecting translation elongation, post-transcriptional transfer RNA (tRNA) modifications, translational termination, and ribosome recycling^{15–17}. Moreover, Cth2 has been shown to repress the translation of specific transcripts in response to Fe deficiency.¹¹ However, changes in protein translation at the genome-wide level and the mechanisms of translational regulation by Fe have not been previously investigated.

In this work, we applied RNA-seq and ribosome profiling (Ribo-Seq) to yeast cells undergoing adaptation to Fe deficiency to quantitatively measure translational changes genome-wide. At the translation level, we uncovered that Fe depletion leads to specific downregulation of genes involved in Fe-dependent processes, including mitochondrial translation and heme biosynthesis. We further show that this translational regulation is mediated by Cth1 and Cth2. We find that Fe deficiency also affects global protein translation by dramatically decreasing the activity of the ribosome recycling factor Rli1. Conversely, eliminating Cth1 and Cth2 increased the levels of Rli1 indicating that cells adapt to Fe deficiency by limiting the activity of Rli1 in response to low Fe in a Cth1/2-dependent manner. Our data also demonstrate that Fe deficiency affects transcription of antisense long non-coding RNAs (lncRNAs) that play a regulatory role by repressing cognate sense mRNA translation. Taken together, this study uncovers the role of the RNA-binding proteins Cth1 and Cth2 in the control of protein translation and how Fe regulates protein synthesis at both global and transcript-specific levels.

RESULTS

Transcriptional and translational responses during the adaptation to iron deficiency

Previous studies have shown that Fe deficiency in yeast *S. cerevisiae* leads to changes in transcriptional profiles^{6,7,18}. In addition, prolonged Fe deficiency has been shown to induce global inhibition of protein synthesis, which is dependent on the Gcn2/eIF2 α pathway.¹⁴ However, little is known about how Fe deprivation manifests at the level of translational regulation. To distinguish the effects of Fe deficiency on mRNA abundance from its effects on protein translation, we performed RNA-seq and ribosome profiling (Ribo-Seq) in wild-type W303a yeast cells cultured in Fe-sufficient (+Fe) or Fe-deficient conditions (-Fe), achieved by the addition of the Fe²⁺-specific chelator bathophenanthroline disulfonate (BPS). For this, exponentially growing cells were isolated under Fe-sufficient conditions, and exposed to a short- (3 h) or long-term (6 h) Fe deficiency (Figure 1A, and Data S1). In addition to wild-type cells, we monitored genome-wide transcriptional and translational changes upon Fe limitation in the *cth1 Δ cth2 Δ* mutant. The RNA-seq and Ribo-Seq profiles showed significantly altered gene expression patterns during adaptation to low Fe from 0 h to 6 h of Fe deficiency, with intermediate changes at 3 h (Figure S1). Consistent with previous studies, we also observed strong inhibition of global protein synthesis after 6 h of Fe deficiency in both wild-type cells and the *cth1 Δ cth2 Δ* mutant as measured by polysome analysis, but changes at 3 h were less pronounced (Figure 1B). We found that most of the changes in translation (Ribo-Seq) during Fe deficiency correlated with the changes in mRNA abundance (RNA-seq) (Figure 1C). Our data demonstrate that the responses to Fe deficiency are mediated primarily by changes in mRNA levels. However, we also found a group of genes that were altered specifically at the translation level indicating that an additional level of regulation contributes to the response of yeast cells to low Fe (Figure 1D). Specifically, we identified 516 upregulated and 428 downregulated genes, respectively, that were altered exclusively at the translation level in wild-type cells during 6 h Fe deficiency (Data S1).

Our analysis of the RNA-seq and Ribo-Seq data revealed many of the previously known changes in response to Fe deficiency. Among the genes transcriptionally upregulated during the time-course of Fe deficiency, we observed a number of Fe regulon genes that are controlled by the Aft1 and Aft2 transcription factors, which validated our experimental approach.^{10,19} Genes upregulated in response to short-term (3 h) Fe limitation were enriched in the GO categories “iron ion homeostasis”, “carboxylic acid metabolic process”, “nucleotide metabolic process”, “siderophore transport”, “cellular amino acid catabolic process”, “carbohydrate metabolic process”, “glycolytic process”, and “response to oxidative stress” (Figures 1E and Data S2). For example, expression of genes involved in Fe siderophore uptake (*FIT1-3*, *ARN1-4*), reductive Fe uptake (*FRE1-FRE4*, *FET3*, *FTR1*, *ATX1*, *CCC2*, and *FET4*), and mobilization of vacuolar Fe (*FRE6*, *FET5*, *FTH1*, and *SMF3*) increased several folds in response to Fe deprivation in wild-type cells (Figure S2). We also observed that the expression levels of *CTH2*, a gene coding for the mRNA-binding protein involved in metabolic remodeling in response to low Fe, were significantly induced in wild-type cells during Fe deficiency. In addition to “iron ion homeostasis” and “carbohydrate metabolic process”, the late response (6 h) to Fe deficiency was associated with upregulation of “autophagy”, “cellular response to external stimulus”, “protein localization to vacuole”, “protein ubiquitination”, “response to nutrient levels”, and “thiamine metabolic process” GO categories.

Among downregulated genes in response to prolonged Fe deficiency (6 h) the most enriched GO categories included “ribosome biogenesis”, “cytoplasmic translation”, and “ribosomal large and small subunits” consistent with the overall inhibition of protein synthesis at this time point. However, there were substantial differences in downregulated genes between wild-type and *cth1 Δ cth2 Δ* cells during both short- (3 h) and long-term (6 h) Fe limitation. For example, “cellular respiration”, “electron transport chain”, “heme biosynthetic process”, “iron-sulfur cluster assembly”, “mitochondrial translation”, and “tricarboxylic acid cycle” were enriched among downregulated genes in wild-type cells, but not in the *cth1 Δ cth2 Δ* mutant. In contrast, “rRNA processing” and “mitotic cell cycle” were specifically downregulated in the *cth1 Δ cth2 Δ* cells suggesting a role of Cth1 and Cth2 in regulation of these processes.

Ribo-Seq analyses reveal the role of the RNA-binding proteins Cth1 and Cth2 in translational regulation

During Fe deficiency, yeast cells activate the expression of Cth2, an mRNA-binding protein involved in the remodeling of Fe metabolism. In response to low Fe, Cth2 and, to a lower extent, Cth1 post-transcriptionally inhibit the expression of several mRNAs that contain AU-rich elements (AREs) in the 3'UTR.^{7,11} We expected that the lack of Cth1 and Cth2 in the *cth1 Δ cth2 Δ* mutant would lead to the derepression of their targets. By comparing changes in actively translated mRNAs (Ribo-Seq) in wild-type and *cth1 Δ cth2 Δ* cells, we identified 164 genes that were

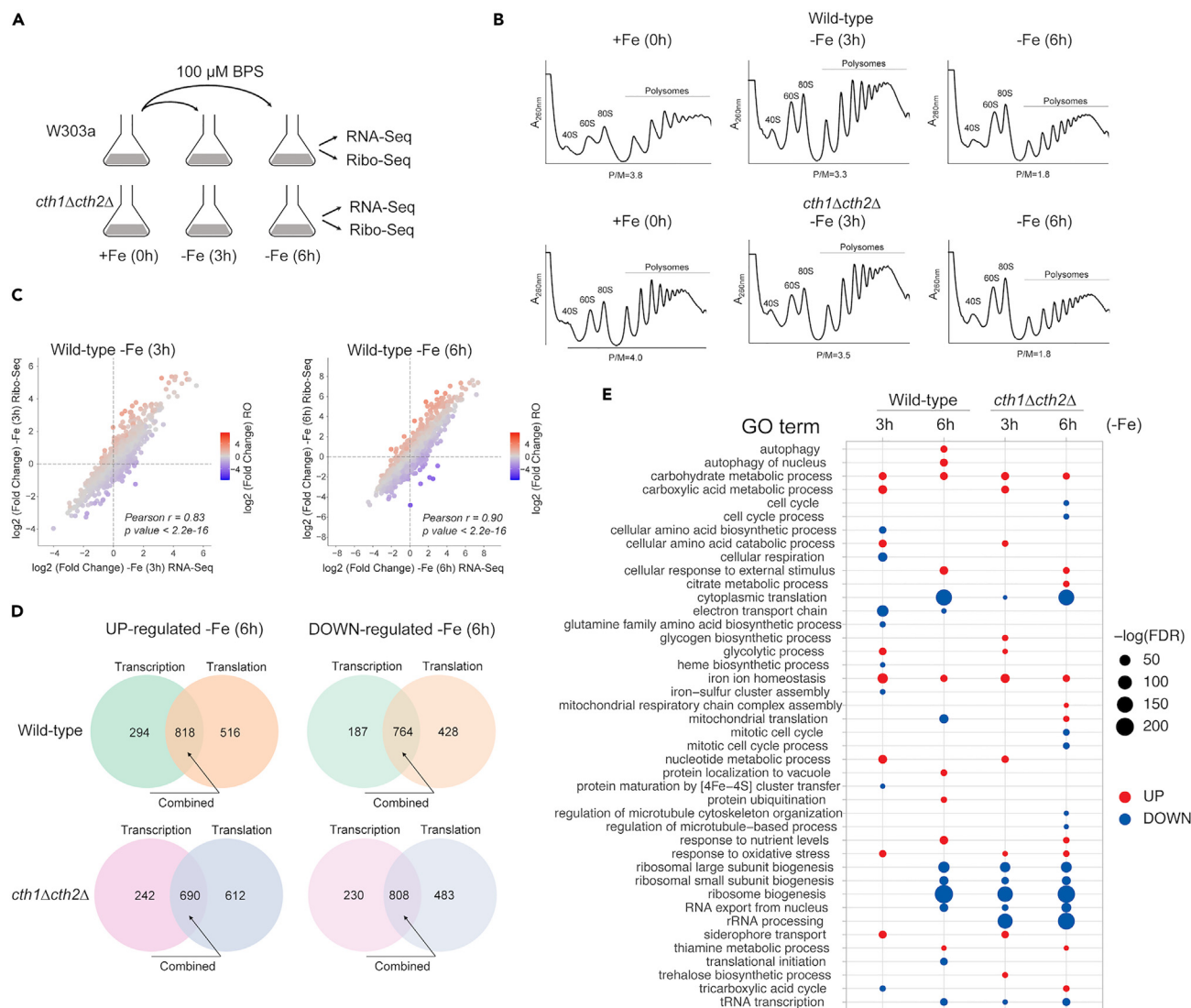


Figure 1. Coordinated changes in mRNA levels and translation allow metabolic reprogramming in response to low Fe

(A) Experimental design.

(B) Polysome profiles of wild-type and *cth1 Δ cth2 Δ* cells during the time-course of Fe deficiency. Polysome to monosome (P/M) ratios were calculated using areas under the curve using ImageJ. Corresponding monosome (40S, 60S, 80S) and polysome peaks are indicated.

(C) Comparison of transcriptional (RNA-seq) and translational (Ribo-Seq) changes during the course of Fe deficiency. Genes whose ribosome occupancy (RO) is increased (red) or decreased (blue) during Fe deficiency are highlighted.

(D) Transcriptional and translational changes in response to Fe deficiency. Venn diagrams show genes that were significantly upregulated or downregulated during 6 h Fe deficiency (FDR<0.05) at the level of mRNA transcription (as quantified by RNA-seq), translation efficiency or a combined effect.

(E) GO terms enriched among translationally up- and downregulated genes during Fe deficiency.

upregulated in the *cth1 Δ cth2 Δ* mutant compared to wild-type cells during 6 h of Fe deficiency (FDR<0.05) (Figure 2A, and Table S1). We further compared changes in ribosomal footprints with changes in RNA abundance allowing us to identify genes that are changed specifically at the translational level. Out of 164 genes upregulated in the *cth1 Δ cth2 Δ* mutant, 153 genes were altered exclusively at the level of protein translation (Figure S3, and Data S1). Among these translationally upregulated genes, we found several previously reported targets of Cth1 and Cth2 that code for components of the electron transport chain (ETC) and tricarboxylic acid (TCA) cycle (Figures 2B and S4), consistent with the known function of Cth1/2 mRNA-binding proteins in post-transcriptional regulation of Fe-dependent genes.^{11,12} In addition to previously described Cth1/2 targets, our data uncovered that Cth1 and Cth2 are limiting the expression of genes encoding for mitochondrial ribosomal proteins (MRPs) (36 ribosomal proteins of the large subunit and 24 ribosomal proteins of the small subunit) as well as proteins involved in the assembly of the ETC (16 genes), mitochondrial translation (15 genes), protein translocation to mitochondria (10 genes), ATP synthase assembly (4 genes), and heme biosynthesis (4 genes) (Figure 2C). Because known targets of Cth1 and Cth2 contain AREs in their

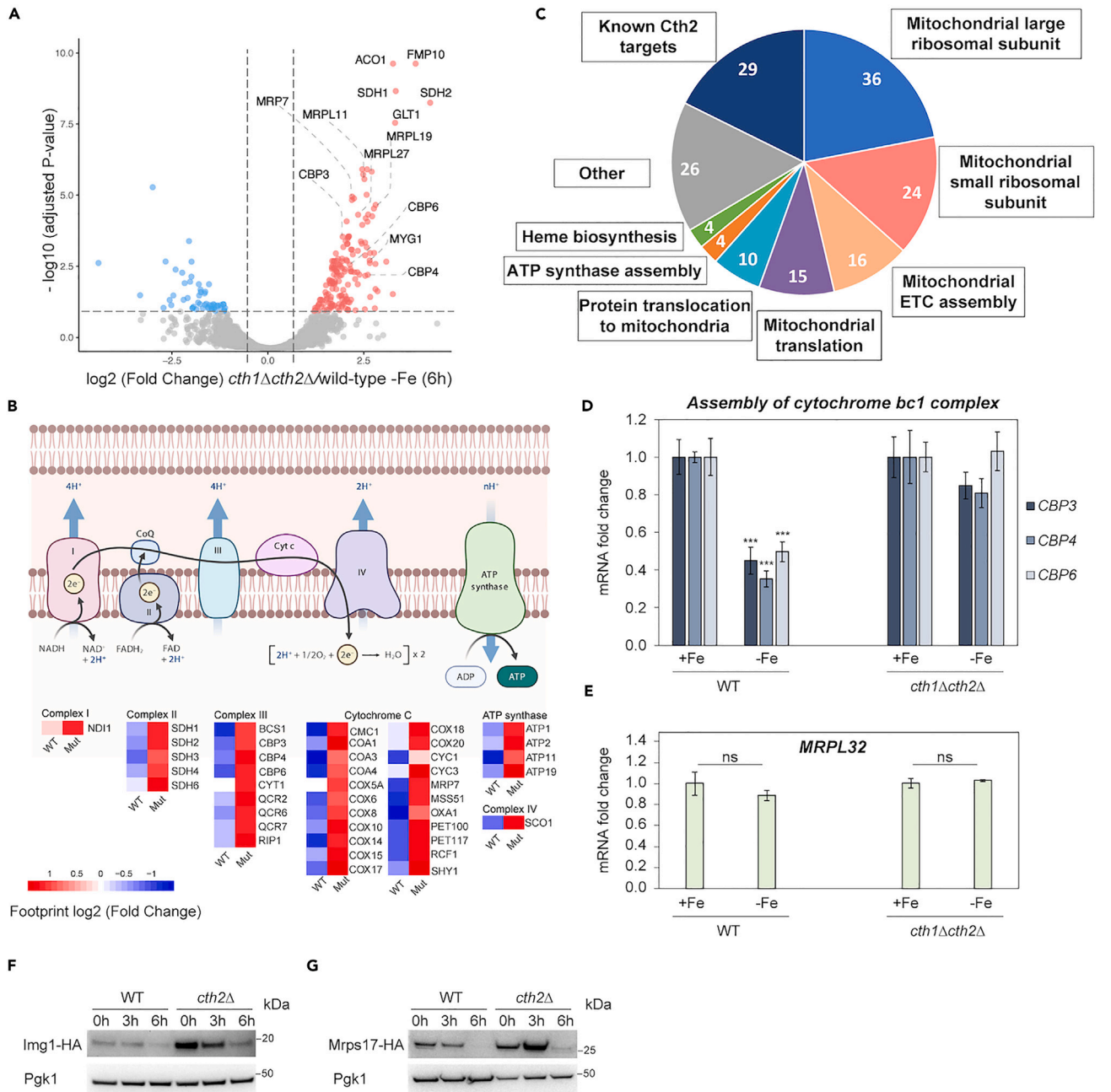


Figure 2. Fe deficiency leads to Cth1/2-dependent inhibition of mitochondrial translation

(A) Volcano plot of differentially regulated genes in the *cth1Δcth2Δ* mutant compared to wild-type cells at 6 h (-Fe).

(B) Heatmap of differentially regulated genes of ETC in *cth1Δcth2Δ* (Mut) compared to wild-type (WT) cells during 6 h of Fe deficiency (FDR<0.05).

(C) Pie chart of genes activated in the *cth1Δcth2Δ* compared to wild-type cells.

(D) Fe deficiency coordinately downregulates expression of transcripts encoding the Cbp3-Cbp4-Cbp6 complex. The expression of *CBP3*, *CBP4*, and *CBP6* was determined by RT-qPCR. Error bars represent SEM of three independent experiments, ****p* < 0.001 (one-way ANOVA).

(E) Translation of mitochondrial ribosomal proteins is regulated by Fe deficiency in a Cth1/2-dependent manner without affecting mRNA transcript levels. The expression of *MRPL32* was determined by RT-qPCR. Error bars represent SEM of three independent experiments, ns, non-significant (one-way ANOVA).

(F–G) Lack of Cth2 in the *cth2Δ* mutant leads to derepression of Img1 (F) and Mrps17 (G) translation. Levels of Img1-HA and Mrps17-HA proteins during Fe deficiency were analyzed by Western blot with anti-HA antibodies. Representative images from two independent experiments are shown.

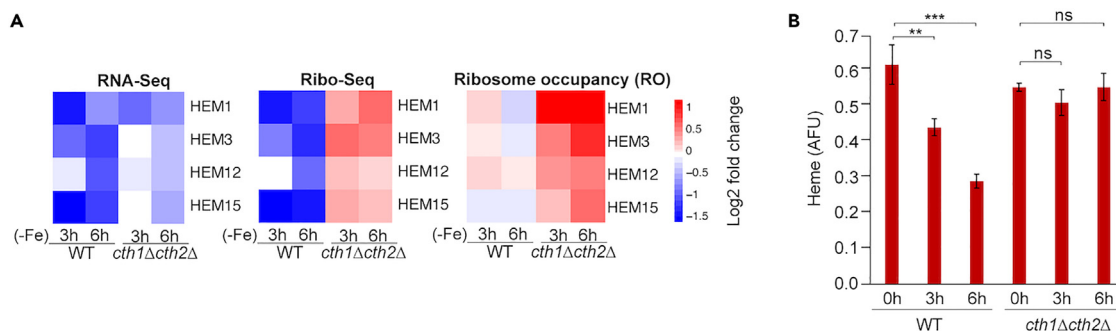


Figure 3. Heme biosynthesis is translationally regulated by Cth1 and Cth2

(A) Heatmaps show log₂ fold change in mRNA abundance (RNA-seq), protein translation (Ribo-Seq), and ribosome occupancy (RO) compared to untreated (0 h) samples.

(B) Intracellular heme levels decreased significantly during Fe deficiency in wild-type cells, whereas it remained constant in the *cth1Δcth2Δ* mutant. Error bars represent SEM of three biological replicates, each containing two technical replicates. ns, non-significant, ***p* < 0.01, ****p* < 0.001 compared with wild-type control (two-way ANOVA).

3'UTR, we searched for putative AREs within 3'UTR of these genes (Table S1). This analysis revealed several transcripts that are directly regulated by Cth1/2. For example, we identified mRNA transcripts encoding the Cbp3-Cbp4-Cbp6 complex, which is involved in the translation and assembly of the mitochondrial cytochrome *bc1* complex²⁰. Our data demonstrate that *CBP3*, *CBP4*, and *CBP6* are coordinately downregulated in response to low Fe in wild-type cells at the mRNA level (but not in the *cth1Δcth2Δ* mutant), suggesting that *CBP3*, *CBP4*, and *CBP6* are directly regulated by Cth1/2 during Fe deficiency (Figure 2D). In contrast, most of the genes encoding for MRP proteins lack AREs in their 3'UTRs and Fe deficiency decreased their translation without affecting their transcript levels (Figures 2E and S5). We also observed that expression of Cth1 and Cth2 is reversely correlated with the synthesis of mitochondrial ribosomal proteins of the small subunit (MRPS) and large subunit (MRPL) during the shift of cells from the fermentable carbon source to the non-fermentable medium containing glycerol (Figure S6) that requires the induction of the mitochondrial ETC components and mitochondrial translation.²¹ Further analysis of MRP genes activated by Fe deficiency in the *cth1Δcth2Δ* mutant identified the presence of Puf3 binding sites in their 3'UTR sequences (Table S1). To validate our findings, we measured the protein levels of two mitochondrial ribosomal proteins, *Img1* and *Mrps17*, regulated by Puf3. Our data show that expression of these targets is downregulated by Fe deficiency. However, the baseline level of both *Img1* and *Mrps17* was significantly higher in the *cth2Δ* mutant compared to wild-type cells (Figures 2F and 2G). These results provide additional support for the role of Cth2 in translational regulation of MRP genes; however, the exact mechanism of this regulation has yet to be investigated.

Notably, we found that Fe deficiency also leads to translational downregulation of genes encoding enzymes involved in heme biosynthesis, including *HEM1*, *HEM3*, *HEM12*, *HEM15* (Figure 3A). To estimate translation efficiency and investigate the contribution of transcriptional and translational regulation to gene expression changes, we calculated ribosome occupancy (RO) for each of these genes. In wild-type cells, both mRNA abundance (RNA-seq) and protein synthesis (Ribo-Seq) of this set of genes were significantly decreased by Fe deficiency (FDR < 0.05). In contrast, translation of *HEM* transcripts was upregulated in the *cth1Δcth2Δ* mutant leading to pronounced increase in RO. To understand whether Cth1 and Cth2 control heme levels, we compared the heme levels in wild-type and *cth1Δcth2Δ* mutant cells subjected to Fe deficiency. We observed a significant decrease in heme levels in wild-type cells after 3 and 6 h of Fe deficiency, whereas the heme levels in the *cth1Δcth2Δ* mutant cells remained constant (Figure 3B). Together, our results indicate that Cth1 and Cth2 play a central role in controlling the changes in protein translation in response to low Fe by directly and indirectly downregulating multiple transcripts required for mitochondrial translation and heme biosynthesis.

Fe deficiency leads to increased ribosome occupancy in the 3'UTRs of genes due to decreased activity of Rli1

Although overall protein synthesis is significantly reduced during Fe deficiency, how different steps of protein translation are affected by low Fe is not completely understood. Among enzymes participating in protein translation that require Fe as a cofactor, we selected Rli1 for further analysis. Rli1 is a conserved protein, which requires an iron-sulfur (Fe-S) cluster for its activity and is essential for translation termination and ribosome recycling.¹⁵ *RLI1* mRNA contains two putative AREs within its 3'UTR at 280 and 291 nt from its stop codon, and its transcript levels are upregulated in cells lacking *CTH1* and *CTH2* as compared to wild-type cells in -Fe conditions^{7,12} suggesting it is a direct Cth1/2 target mRNA. We expected that, during Fe deficiency, activity of Rli1 would decrease leading to the increased translation of 3'UTR sequences.¹⁶ To test this, we performed genome-wide quantification of Ribo-Seq reads that aligned to 3'UTR of all annotated genes. We identified numerous 3'UTRs with increased ribosome occupancy in response to Fe deficiency compared to untreated wild-type cells, including *SED1* and *CWP2*, known targets of Rli1 (Figure S7). Consistent with the function of Rli1 in ribosome recycling, we observed increased accumulation of 80S ribosomes in the 3'UTRs of *SED1* during prolonged Fe deficiency (6 h) in wild-type cells (Figure 4A). In contrast, the decrease in activity of Rli1 was delayed in the *cth1Δcth2Δ* mutant. To investigate whether increased ribosome occupancy at 3'UTR in Fe-depleted conditions is associated with active translation, we used yeast strains containing 3xHA tags in the 3'UTRs of *SED1* and *CWP2*¹⁶ downstream of the canonical stop codon. We

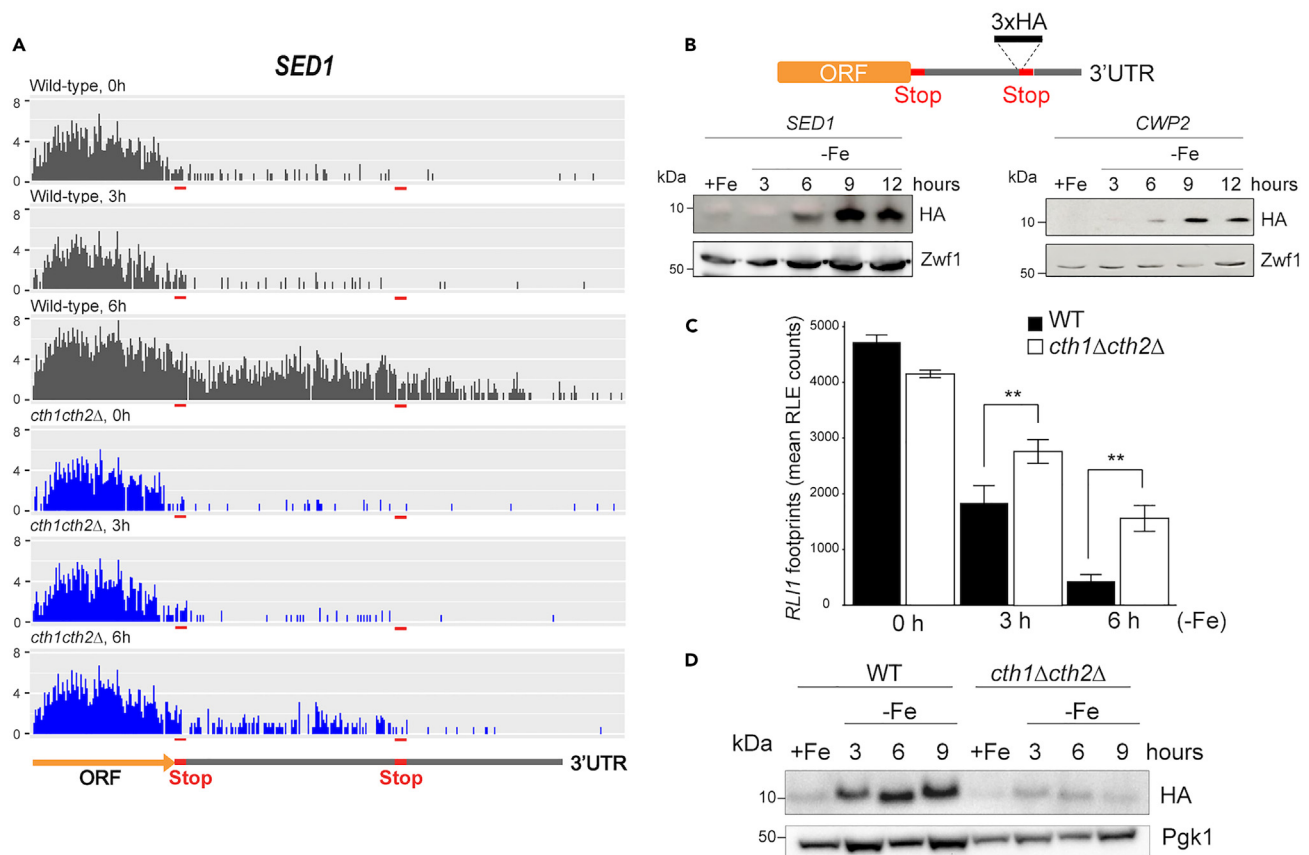


Figure 4. Fe deficiency leads to increased translation of 3'UTRs due to Cth1/2-dependent inhibition of Rli1 activity

(A) Ribosome occupancy at the 3'UTR of *SED1* mRNA during short (3 h) and prolonged (6 h) Fe deficiency (-Fe). The location of the translation termination site is shown with red boxes.

(B) Strains containing 3xHA tags inserted in the 3'UTRs of *SED1* and *CWP2*¹⁶ show increased translation downstream of the canonical translation stop codon during prolonged Fe deficiency. The expression of tagged proteins was detected by Western blot analysis with HA-tag antibody. Given the size of 4.8 kDa for 3xHA tag, the observed MWs ~7–10 kDa of the bands correspond to the production of small 3'UTR translation products (~2–5 kDa).

(C) Lack of Cth1/2 in the *cth1Δcth2Δ* mutant leads to derepression of *RLI1*. Changes in *RLI1* expression in response to Fe deficiency were calculated by analyzing the number of footprints (RLE normalized counts) in the Ribo-Seq dataset generated in our study. Error bars represent SEM of three independent experiments, ** $p < 0.01$ (one-way ANOVA).

(D) Expression of the *CWP2* 3'UTR translation product is prevented in the *cth1Δcth2Δ* mutant.

observed increased levels of 3'UTR translation products for *SED1* and *CWP2* genes during prolonged incubation of wild-type cells in the absence of Fe (Figure 4B). Western blot analysis revealed that these bands correspond to the production of small peptide products (~2–5 kDa), rather than readthrough translation products that are expected to have larger sizes. Notably, eliminating Cth1 and Cth2 prevented their repressive effects on the expression levels of *RLI1* during Fe deficiency in the *cth1Δcth2Δ* mutant (Figure 4C) lowering expression of the *CWP2* 3'UTR translation product (Figure 4D). Together, these data suggest that Fe deficiency decreases activity of Rli1 by promoting binding of Cth1/2 to the AREs in its 3'UTR and promoting degradation of its transcript.

MRS3 translation is repressed by antisense transcription of a long non-coding RNA

Among the genes translationally regulated by Fe deficiency, we identified *MRS3* that encodes a mitochondrial Fe transporter. Footprint coverage of *MRS3* was downregulated in response to Fe deficiency suggesting reduced translation of this gene in low Fe conditions (Figure 5A, right panel). But at the RNA level, we observed increased expression of an antisense long non-coding RNA (lncRNA), which we named *MRS3*^{AS} (Figure 5A, left panel). We further confirmed increased expression of the *MRS3*^{AS} antisense transcript using RT-qPCR during prolonged Fe deficiency (Figure 5B), which was associated with 9.2-fold reduction of the Mrs3 protein levels (Figure 5C). In contrast to *MRS3*, low Fe did not affect footprint coverage of its homolog *MRS4*, and we did not observe expression of the antisense RNA for this gene (Figure S8A). We then asked whether increased expression of the *MRS3*^{AS} transcript is dependent on Cth1 and Cth2. However, we observed increased *MRS3*^{AS} transcription in response to low Fe in the *cth1Δcth2Δ* mutant (Figure S8B) indicating that Fe deficiency regulates Mrs3

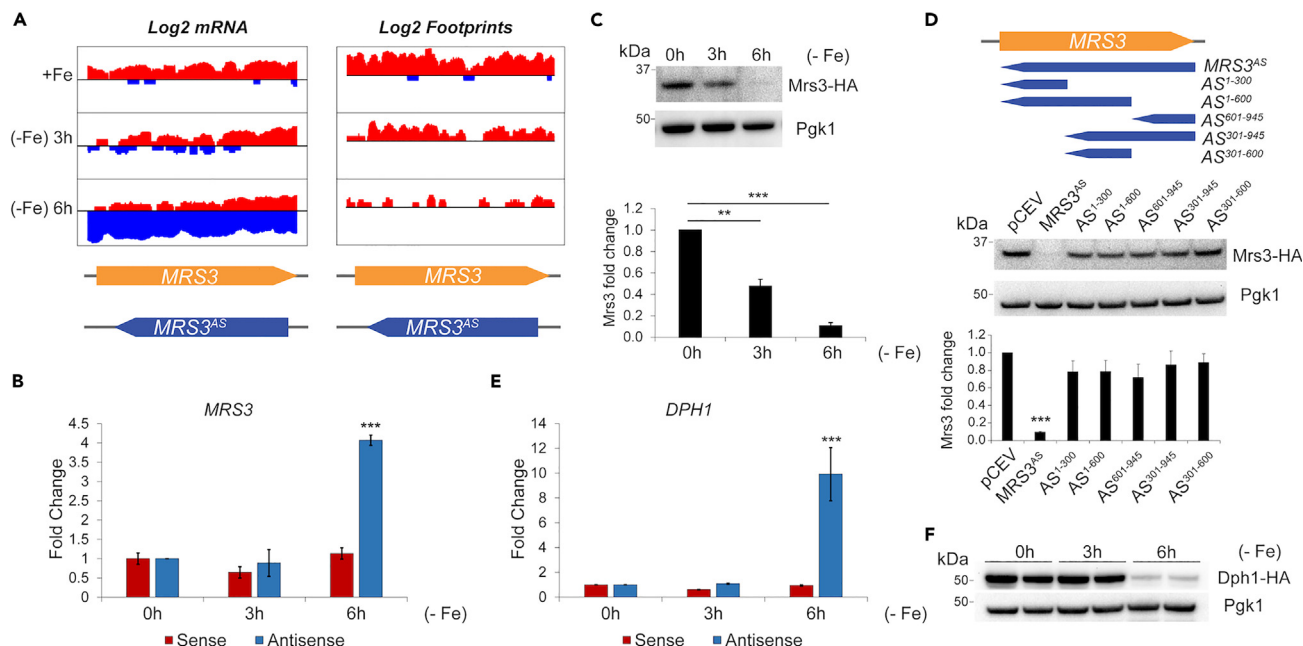


Figure 5. Fe deficiency induces expression of regulatory lncRNAs

(A) Coverage plot of reads mapped to sense (red) and antisense (blue) *MRS3* transcript. Y axis represents log₂ transformed number of reads, x axis coordinates show nucleotide positions within *MRS3* ORF.

(B) Expression of antisense *MRS3* (*MRS3^{AS}*) transcript is significantly upregulated upon Fe deficiency. Relative expression of *MRS3* and *MRS3^{AS}* transcripts was analyzed by RT-qPCR. Error bars represent SEM of three independent experiments, ****p* < 0.001 (two-way ANOVA).

(C) *Mrs3* protein levels are repressed by prolonged Fe deficiency. Expression of *Mrs3*-HA and Pgk1 proteins was determined by Western blot with anti-HA and anti-Pgk1 antibodies, respectively. Error bars represent SEM of three independent experiments, ***p* < 0.01, ****p* < 0.001 (t test).

(D) Expression of *MRS3^{AS}* lncRNA is sufficient to repress translation of *MRS3*. Cells expressing HA-tagged *Mrs3* protein were transformed with either an empty vector (pCEV) or pCEV-*MRS3^{AS}* expressing full length (*MRS3^{AS}*) or short forms of the antisense *MRS3* transcript (AS) and *Mrs3* protein levels were analyzed by Western blot. Error bars represent SEM of three independent experiments, ****p* < 0.001 (t test).

(E) Relative expression of *DPH1* and *DPH1^{AS}* transcripts was analyzed by RT-qPCR. Error bars represent SEM of three independent experiments, ****p* < 0.001 (two-way ANOVA).

(F) Expression of *Dph1*-HA protein during Fe deficiency was analyzed by Western blot with anti-HA antibodies.

levels in a Cth1/2-independent manner. Finally, to determine if *MRS3^{AS}* transcription is sufficient for the repression of *MRS3*, we generated a plasmid expressing antisense lncRNA. Expression of the full length *MRS3^{AS}* lncRNA, but not its shorter forms, decreased *Mrs3* protein translation in the absence of Fe deficiency (Figure 5D) suggesting that ectopic expression of the antisense lncRNA is sufficient to repress protein translation.

Expression of antisense lncRNAs is a conserved regulatory mechanism in yeast

As *MRS3* is translationally regulated by an antisense lncRNA, we asked if other genes might be controlled by low Fe using a similar mechanism. We searched for the presence of antisense lncRNA transcription in other genes that are translationally downregulated by Fe deficiency. For this, we systematically searched for *cis*-antisense transcripts, which overlap protein coding genes and are transcribed from the opposite DNA strand, leading to decreased sense mRNA translation. Using our pipeline, we identified 42 putative mRNA:lncRNA pairs, which had more than a 2-fold increase in expression of antisense transcripts during 6 h Fe deficiency (Data S3). In addition to *MRS3*, we identified *DPH1*, an Fe-S cluster-containing protein implicated in diphthamide modification of eukaryotic elongation factor 2 (eEF2), which showed increased antisense transcription following 6 h of Fe deficiency (Figure S8C), leading to significant decrease of *DPH1* footprint coverage. Using RT-qPCR, we further confirmed the increased expression of the antisense lncRNA (*DPH1^{AS}*) during prolonged Fe deprivation (Figure 5E), which was associated with decreased translation of the main ORF transcript and decreased levels of *Dph1* protein (Figure 5F). The observation that translation of both *MRS3* and *DPH1* are repressed by low Fe suggests that this may be a conserved regulatory mechanism.

DISCUSSION

Although transcriptional responses to Fe deprivation have been extensively characterized, how Fe deficiency affects protein synthesis at the genome-wide level remained elusive. By combining RNA-seq with the analysis of ribosome occupancy by Ribo-Seq, we quantitatively analyzed translational changes in response to the short-term and prolonged Fe deficiency in yeast. This allowed us to identify groups of genes

whose expression was specifically altered by low Fe either at the transcriptional or protein synthesis level, providing mechanistic insights into the role of Fe in protein translation.

The changes in gene expression that we observed were consistent with prior studies that analyzed transcriptomic profiles during Fe deprivation showing altered expression of genes involved in Fe acquisition and mobilization.^{6,7} Expression of these genes is activated by the Aft1 and Aft2 transcription factors. In addition, we observed that Cth1 and Cth2 mRNA-binding proteins repress expression of their targets adjusting metabolism to prioritize Fe for essential processes.¹⁹ For most of the transcripts, a strong correlation between RNA-seq and Ribo-Seq profiles was found indicating that changes in gene expression induced by Fe deficiency predominantly occur at the mRNA level. However, we also identified a number of genes that were specifically downregulated by Fe deficiency at the translation level. These downregulated proteins included enzymes involved in heme biosynthesis as well as mitochondrial ribosomal proteins and other components of the mitochondrial translational machinery. Importantly, we identified Cth1 and Cth2 as key factors that are responsible for this translational repression. Although *HEM15* was already identified as a target of translational repression by Cth2 in our previously published study,¹¹ we now show that Cth1/2-mediated translational repression of heme biosynthesis genes and inhibition of mitochondrial translation contribute to reducing heme levels in response to Fe deficiency.

Although the exact mechanisms of translational regulation by Cth1 and Cth2 remain unclear, we found that many of the genes translationally downregulated by Cth1/2 contained binding sites for the Puf3 RNA-binding protein in their 3'UTRs. Puf3 is a known regulator of mitochondrial translation in response to glucose availability, which specifically binds to mRNA and represses translation of mitochondrial ribosomal proteins (MRPs).^{22,23} In glucose-replete conditions, Puf3 degrades mRNA of MRPs limiting mitochondrial translation,^{24,25} which aligns with known metabolism preferences of yeast for glucose utilization through fermentation. In contrast, glucose depletion or switch to non-fermentable carbon sources leads to Puf3 phosphorylation and the subsequent switch of its function from mRNA degradation to the facilitation of translation.²⁶ Our data indicate that expression of Cth1 and Cth2 is inversely correlated with the levels of mitochondrial ribosomal proteins during the transition of yeast cells from high glucose media to media containing glycerol further supporting the role of Cth1 and Cth2 in regulation of mitochondrial translation. Nonfermentable carbon sources, such as glycerol, require expression of the components of the oxidative phosphorylation and active mitochondrial translation,²⁷ suggesting that the activity of Cth1/2 and Puf3 may allow proper synchronization between mitochondrial translation and Fe levels, and that this regulation is not only involved in acute response to Fe deficiency, but may also play a role in physiological, homeostatic processes. Supporting this idea, we recently found that increased expression of Cth2 is limiting the expression of mitochondrial ribosomal proteins during yeast replicative aging.²⁸

Another effect of Fe deficiency on translation was identified when 3'UTR sequences were analyzed. Ribosome profiling of Fe-depleted cells revealed a striking decrease in the activity of the Fe-S cluster-containing Rli1 protein that serves as a ribosome recycling factor. We show that the number of footprints mapped to 3'UTR sequences was increased in Fe-deficient conditions to the same extent as seen previously in Rli1-depleted yeast cells¹⁶ leading to the generation of aberrant 3'UTR translation products. Notably, we observed a delayed response in the *cth1Δcth2Δ* mutant indicating that Fe deficiency represses Rli1 function in wild-type cells as a result of Cth1/2-mediated post-transcriptional downregulation of *RLI1* transcripts. These data suggest that yeast cells deliberately downregulate the abundance of *RLI1* mRNA through Cth1 and Cth2 to limit Fe utilization by Rli1.

Finally, our study uncovered an important role of antisense lncRNA in the translational regulation of specific mRNA transcripts in response to low Fe. Our data demonstrate that Fe deficiency leads to increased expression of the regulatory antisense *MRS3* transcript repressing translation of cognate mRNA. Moreover, overexpression of the antisense lncRNA is sufficient to repress *Mrs3* translation. Additionally, we found that Dph1, an Fe-S cluster-containing protein that participates in the first step of diphthamide modification of eEF2, is also regulated by a lncRNA. Diphthamide modification of eEF2 is important for efficient ribosome translocation and translational fidelity during protein synthesis.¹⁵ Together, these observations suggest a possible mechanism for the role of Fe in global regulation of protein translation and highlight the complexity of the cellular adaptation to low Fe. Recent genome-wide studies identified a number of genes that have overlapping antisense RNA transcripts in yeast and in other species^{29–31} raising a possibility that expression of lncRNAs may have a role in Fe-dependent regulation of gene expression in higher eukaryotes. Additionally, regulation of protein translation by antisense transcripts has been implicated in several human diseases including cancer, cardiovascular and muscular pathologies, neurodegenerative disorders, and diabetes.³² It would be interesting to examine the importance of lncRNA-mediated translational repression in response to Fe deficiency in these pathophysiological processes.

Limitations of the study

Together, our findings uncovered a complex effect of Fe deficiency on the regulation of protein synthesis showing how this important metal affects protein translation at multiple levels (Figure 6). However, several important questions remain. First, the mechanism by which Cth1 and Cth2 affect translation of mitochondrial ribosomal proteins and the role of Puf3 in this process warrant further investigation. Second, the mechanism of *Mrs3* translation inhibition by antisense lncRNA is not completely understood. Future studies will be focused on studying the mechanism underlying the transcriptional activation of *MRS3^{AS}* during periods of Fe deficiency, examining the impact of prolonged Fe deficiency on the transcription of lncRNAs, and gaining a deeper understanding of how this regulatory mechanism contributes to cellular adaptation to Fe deficiency. In this paper we employed a quantitative approach to analyze genome-wide changes in ribosome occupancy of actively translated mRNAs during Fe deficiency in yeast. Nevertheless, the role of mammalian counterparts of Cth2 in regulating protein translation and responding to Fe deficiency remains to be elucidated. Given that many essential Fe-containing enzymes have been implicated in several steps of protein translation in mammals,¹⁵ the principles of Fe-dependent translational regulation uncovered in yeast may shed light on mechanisms that control protein synthesis in higher eukaryotes.

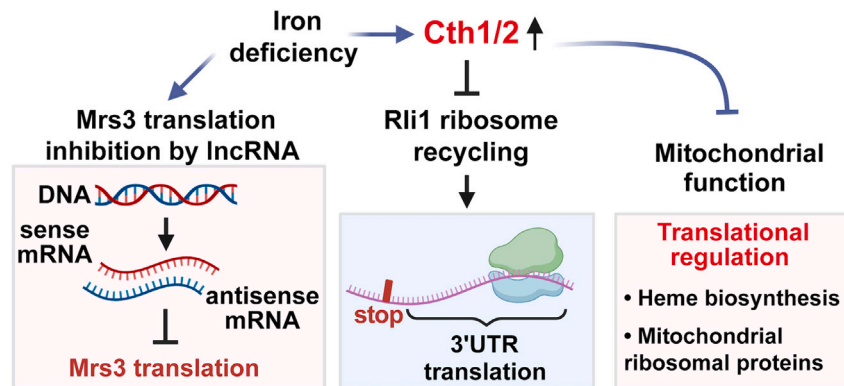


Figure 6. Model for the role of yeast RNA-binding proteins Cth1 and Cth2 in the control of protein translation during adaptation to Fe deficiency.

STAR★METHODS

Detailed methods are provided in the online version of this paper and include the following:

- KEY RESOURCES TABLE
- RESOURCE AVAILABILITY
 - Lead contact
 - Materials availability
 - Data and code availability
- EXPERIMENTAL MODEL AND STUDY PARTICIPANT DETAILS
 - Yeast strains
- METHOD DETAILS
 - Ribo-Seq and RNA-seq sequencing, data processing, and analysis
 - Ribosome occupancy analysis
 - Quantification of antisense transcripts
 - Polysome analysis
 - RT-qPCR
 - Western blot analysis
 - Expression of the *MRS3^{AS}* lncRNA
 - Heme quantification
- QUANTIFICATION AND STATISTICAL ANALYSIS

SUPPLEMENTAL INFORMATION

Supplemental information can be found online at <https://doi.org/10.1016/j.isci.2024.109868>.

ACKNOWLEDGMENTS

We would like to thank Dr. Alan Hinnebusch for providing yeast strains containing 3xHA tags in the 3'UTRs of *SED1* and *CWP2* and Dr. Stirling Churchman for providing *Img1-3xHA* and *Mrps17-3xHA* strains used in this study. This work was supported by NIH grants AG058713 and AG066704 to V.M.L., and grants PID2020-116940RB-I00 and CEX2021-001189-S from MCIN/AEI/10.13039/501100011033 to S.P. V.N.G. was supported by NIA grants.

AUTHOR CONTRIBUTIONS

H.B. and V.M.L. designed the study. H.B., A.M.R., A.G., and P.K.P. performed experiments. H.B., A.M.R., A.G., P.K.P., A.T., M.T.M.-P., V.N.G., S.P., and V.M.L. analyzed the data. H.B. and V.M.L. wrote the original manuscript. All authors edited the paper.

DECLARATION OF INTERESTS

The authors declare no competing interests.

Received: September 28, 2023

Revised: March 12, 2024

Accepted: April 29, 2024

Published: April 30, 2024

REFERENCES

- Zhang, C. (2014). Essential functions of iron-requiring proteins in DNA replication, repair and cell cycle control. *Protein Cell* 5, 750–760. <https://doi.org/10.1007/s13238-014-0083-7>.
- Andrews, N.C. (2000). Iron Metabolism: Iron Deficiency and Iron Overload. *Annu. Rev. Genomics Hum. Genet.* 1, 75–98. <https://doi.org/10.1146/annurev.genom.1.1.75>.
- Cronin, S.J.F., Woolf, C.J., Weiss, G., and Penninger, J.M. (2019). The Role of Iron Regulation in Immunometabolism and Immune-Related Disease. *Front. Mol. Biosci.* 6, 116. <https://doi.org/10.3389/fmolb.2019.00116>.
- Hare, D., Ayton, S., Bush, A., and Lei, P. (2013). A delicate balance: Iron metabolism and diseases of the brain. *Front. Aging Neurosci.* 5, 34. <https://doi.org/10.3389/fnagi.2013.00034>.
- Xu, J., Jia, Z., Knutson, M.D., and Leeuwenburgh, C. (2012). Impaired Iron Status in Aging Research. *Int. J. Mol. Sci.* 13, 2368–2386.
- Shakoury-Elizeh, M., Tiedeman, J., Rashford, J., Ferea, T., Demeter, J., Garcia, E., Rolfes, R., Brown, P.O., Botstein, D., and Philpott, C.C. (2004). Transcriptional remodeling in response to iron deprivation in *Saccharomyces cerevisiae*. *Mol. Biol. Cell* 15, 1233–1243. <https://doi.org/10.1091/mbc.e03-09-0642>.
- Puig, S., Askeland, E., and Thiele, D.J. (2005). Coordinated remodeling of cellular metabolism during iron deficiency through targeted mRNA degradation. *Cell* 120, 99–110. <https://doi.org/10.1016/j.cell.2004.11.032>.
- Romero, A.M., Ramos-Alonso, L., Montellá-Manuel, S., García-Martínez, J., de la Torre-Ruiz, M.A., Pérez-Ortín, J.E., Martínez-Pastor, M.T., and Puig, S. (2019). A genome-wide transcriptional study reveals that iron deficiency inhibits the yeast TORC1 pathway. *Biochim. Biophys. Acta. Gene Regul. Mech.* 1862, 194414. <https://doi.org/10.1016/j.bbagr.2019.194414>.
- Philpott, C.C., and Protchenko, O. (2008). Response to iron deprivation in *Saccharomyces cerevisiae*. *Eukaryot. Cell* 7, 20–27. <https://doi.org/10.1128/EC.00354-07>.
- Ramos-Alonso, L., Romero, A.M., Martínez-Pastor, M.T., and Puig, S. (2020). Iron Regulatory Mechanisms in *Saccharomyces cerevisiae*. *Front. Microbiol.* 11, 582830. <https://doi.org/10.3389/fmicb.2020.582830>.
- Ramos-Alonso, L., Romero, A.M., Soler, M.À., Perea-García, A., Alepuz, P., Puig, S., and Martínez-Pastor, M.T. (2018). Yeast Cth2 protein represses the translation of ARE-containing mRNAs in response to iron deficiency. *PLoS Genet.* 14, e1007476. <https://doi.org/10.1371/journal.pgen.1007476>.
- Puig, S., Vergara, S.V., and Thiele, D.J. (2008). Cooperation of two mRNA-binding proteins drives metabolic adaptation to iron deficiency. *Cell Metab.* 7, 555–564. <https://doi.org/10.1016/j.cmet.2008.04.010>.
- Sanvisens, N., Baño, M.C., Huang, M., and Puig, S. (2011). Regulation of ribonucleotide reductase in response to iron deficiency. *Mol. Cell* 44, 759–769. <https://doi.org/10.1016/j.molcel.2011.09.021>.
- Romero, A.M., Ramos-Alonso, L., Alepuz, P., Puig, S., and Martínez-Pastor, M.T. (2020). Global translational repression induced by iron deficiency in yeast depends on the Gcn2/eIF2alpha pathway. *Sci. Rep.* 10, 233. <https://doi.org/10.1038/s41598-019-57132-0>.
- Romero, A.M., Martínez-Pastor, M.T., and Puig, S. (2021). Iron in Translation: From the Beginning to the End. *Microorganisms* 9. <https://doi.org/10.3390/microorganisms9051058>.
- Young, D.J., Guydosh, N.R., Zhang, F., Hinnebusch, A.G., and Green, R. (2015). Rli1/ABCE1 Recycles Terminating Ribosomes and Controls Translation Reinitiation in 3'UTRs In Vivo. *Cell* 162, 872–884. <https://doi.org/10.1016/j.cell.2015.07.041>.
- Keeling, K.M., Salas-Marco, J., Osheroovich, L.Z., and Bedwell, D.M. (2006). Tpa1p is part of an mRNP complex that influences translation termination, mRNA deadenylation, and mRNA turnover in *Saccharomyces cerevisiae*. *Mol. Cell Biol.* 26, 5237–5248. <https://doi.org/10.1128/MCB.02448-05>.
- Hausmann, A., Samans, B., Lill, R., and Mühlenhoff, U. (2008). Cellular and mitochondrial remodeling upon defects in iron-sulfur protein biogenesis. *J. Biol. Chem.* 283, 8318–8330. <https://doi.org/10.1074/jbc.M705570200>.
- Philpott, C.C., Leidgens, S., and Frey, A.G. (2012). Metabolic remodeling in iron-deficient fungi. *Biochim. Biophys. Acta* 1823, 1509–1520. <https://doi.org/10.1016/j.bbamcr.2012.01.012>.
- Gruschke, S., Römpler, K., Hildenbeutel, M., Kehrein, K., Kühl, I., Bonnefoy, N., and Ott, M. (2012). The Cbp3-Cbp6 complex coordinates cytochrome b synthesis with bc(1) complex assembly in yeast mitochondria. *J. Cell Biol.* 199, 137–150. <https://doi.org/10.1083/jcb.201206040>.
- Isaac, R.S., McShane, E., and Churchman, L.S. (2018). The Multiple Levels of Mitonuclear Coregulation. *Annu. Rev. Genet.* 52, 511–533. <https://doi.org/10.1146/annurev-genet-120417-031709>.
- Gerber, A.P., Herschlag, D., and Brown, P.O. (2004). Extensive association of functionally and topologically related mRNAs with Puf family RNA-binding proteins in yeast. *PLoS Biol.* 2, E79. <https://doi.org/10.1371/journal.pbio.0020079>.
- Lapointe, C.P., Stefely, J.A., Jochem, A., Hutchins, P.D., Wilson, G.M., Kwicien, N.W., Coon, J.J., Wickens, M., and Pagliarini, D.J. (2018). Multi-omics Reveal Specific Targets of the RNA-Binding Protein Puf3p and Its Orchestration of Mitochondrial Biogenesis. *Cell Syst.* 6, 125–135.e6. <https://doi.org/10.1016/j.cels.2017.11.012>.
- Houshmandi, S.S., and Olivas, W.M. (2005). Yeast Puf3 mutants reveal the complexity of Puf-RNA binding and identify a loop required for regulation of mRNA decay. *RNA* 11, 1655–1666. <https://doi.org/10.1261/rna.2168505>.
- Olivas, W., and Parker, R. (2000). The Puf3 protein is a transcript-specific regulator of mRNA degradation in yeast. *EMBO J.* 19, 6602–6611. <https://doi.org/10.1093/emboj/19.23.6602>.
- Lee, C.D., and Tu, B.P. (2015). Glucose-Regulated Phosphorylation of the PUF Protein Puf3 Regulates the Translational Fate of Its Bound mRNAs and Association with RNA Granules. *Cell Rep.* 11, 1638–1650. <https://doi.org/10.1016/j.celrep.2015.05.014>.
- Couvillion, M.T., Soto, I.C., Shipkovenska, G., and Churchman, L.S. (2016). Synchronized mitochondrial and cytosolic translation programs. *Nature* 533, 499–503. <https://doi.org/10.1038/nature18015>.
- Patnaik, P.K., Beupere, C., Barlit, H., Romero, A.M., Tsuchiya, M., Muir, M., Martínez-Pastor, M.T., Puig, S., Kaeberlein, M., and Labunsky, V.M. (2022). Deficiency of the RNA-binding protein Cth2 extends yeast replicative lifespan by alleviating its repressive effects on mitochondrial function. *Cell Rep.* 40, 111113. <https://doi.org/10.1016/j.celrep.2022.111113>.
- Zhao, X., Li, J., Lian, B., Gu, H., Li, Y., and Qi, Y. (2018). Global identification of Arabidopsis lncRNAs reveals the regulation of MAF4 by a natural antisense RNA. *Nat. Commun.* 9, 5056. <https://doi.org/10.1038/s41467-018-07500-7>.
- Liu, S.J., Horlbeck, M.A., Cho, S.W., Birk, H.S., Malatesta, M., He, D., Attenello, F.J., Villalta, J.E., Cho, M.Y., Chen, Y., et al. (2017). CRISPRi-based genome-scale identification of functional long noncoding RNA loci in human cells. *Science* 355, aah7111. <https://doi.org/10.1126/science.aah7111>.
- Till, P., Mach, R.L., and Mach-Aigner, A.R. (2018). A current view on long noncoding RNAs in yeast and filamentous fungi. *Appl. Microbiol. Biotechnol.* 102, 7319–7331. <https://doi.org/10.1007/s00253-018-9187-y>.
- Barman, P., Reddy, D., and Bhaumik, S.R. (2019). Mechanisms of Antisense Transcription Initiation with Implications in Gene Expression, Genomic Integrity and Disease Pathogenesis. *Noncoding RNA* 5, 11. <https://doi.org/10.3390/ncrna5010011>.
- Dobin, A., Davis, C.A., Schlesinger, F., Drenkow, J., Zaleski, C., Jha, S., Batut, P., Chaisson, M., and Gingeras, T.R. (2013). STAR: ultrafast universal RNA-seq aligner. *Bioinformatics* 29, 15–21. <https://doi.org/10.1093/bioinformatics/bts635>.
- Liao, Y., Smyth, G.K., and Shi, W. (2019). The R package Rsubread is easier, faster, cheaper and better for alignment and quantification of RNA sequencing reads.

- Nucleic Acids Res. 47, e47. <https://doi.org/10.1093/nar/gkz114>.
35. Robinson, M.D., McCarthy, D.J., and Smyth, G.K. (2010). edgeR: a Bioconductor package for differential expression analysis of digital gene expression data. *Bioinformatics* 26, 139–140. <https://doi.org/10.1093/bioinformatics/btp616>.
36. Ritchie, M.E., Phipson, B., Wu, D., Hu, Y., Law, C.W., Shi, W., and Smyth, G.K. (2015). limma powers differential expression analyses for RNA-sequencing and microarray studies. *Nucleic Acids Res.* 43, e47. <https://doi.org/10.1093/nar/gkv007>.
37. Barre, B.P., Hallin, J., Yue, J.X., Persson, K., Mikhalev, E., Irizar, A., Holt, S., Thompson, D., Molin, M., Warringer, J., and Liti, G. (2020). Intragenic repeat expansion in the cell wall protein gene HPP1 controls yeast chronological aging. *Genome Res.* 30, 697–710. <https://doi.org/10.1101/gr.253351.119>.
38. Beaupere, C., Chen, R.B., Pelosi, W., and Labunskyy, V.M. (2017). Genome-wide quantification of translation in budding yeast by ribosome profiling. *J. Vis. Exp.* 130, e56820. <https://doi.org/10.3791/56820>.
39. Martin, M. (2011). Cutadapt Removes Adapter Sequences from High-Throughput Sequencing Reads. *EMBnet J.* 17, 3. <https://doi.org/10.14806/ej.17.1.200>.
40. Anders, S., and Huber, W. (2010). Differential expression analysis for sequence count data. *Genome Biol.* 11, R106. <https://doi.org/10.1186/gb-2010-11-10-r106>.
41. Vickers, C.E., Bydder, S.F., Zhou, Y., and Nielsen, L.K. (2013). Dual gene expression cassette vectors with antibiotic selection markers for engineering in *Saccharomyces cerevisiae*. *Microb. Cell Fact.* 12, 96. <https://doi.org/10.1186/1475-2859-12-96>.

STAR★METHODS

KEY RESOURCES TABLE

REAGENT or RESOURCE	SOURCE	IDENTIFIER
Antibodies		
HA Tag Monoclonal Antibody (2–2.2.14), HRP (1 mg/mL)	ThermoFisher	Cat#26183-HRP; RRID: AB_2533056
Bacterial and virus strains		
DH5-alpha Competent <i>E. coli</i> (High Efficiency)	New England Biolabs	Cat#C2987H
Chemicals, peptides, and recombinant proteins		
Yeast Extract	Research Products International	SKU: Y20020
Peptone	Research Products International	SKU: P20250
D-(+)-Glucose	Research Products International	SKU: G32040
Glycerol	Research Products international	SKU: G22025–0.5; CAS: 56-81-5
Agar	Sunrise Science Products	Cat#1910-500
CSM-Ura Powder	Sunrise Science Products	Cat#1004-010
Yeast Nitrogen Base	Research Products International	SKU: Y20040
G418 Sulfate	Corning	Cat#30-234-CR
Nourseothricin sulfate (NAT)	GoldBio	Cat#N500
Ampicillin, Sodium Salt	Research Products International	SKU: A40040–5.0
D-(+)-Galactose	Research Products International	SKU: G33000
Phusion High-Fidelity DNA Polymerase	New England Biolabs	Cat#M0530S
10 mM dNTP mix	ThermoFisher	Cat#R0191
E.Z.N.A. Gel Extraction Kit	Omega Bio-tek	SKU: D2500-01
KAPA SYBR FAST qPCR Master Mix (2X) Universal	Kapa Biosystems	Cat#KK4601
SuperScript III Reverse Transcriptase	ThermoFisher	Cat#18080093
T4 DNA ligase	New England Biolabs	Cat#M0202S
EZ-10 Spin Column Plasmid DNA Miniprep Kit	BioBasic	Cat#BS413
Lithium acetate	ThermoFisher	Cat#AC297110250
Polyethylene glycol 3000 (PEG 3000)	Sigma-Aldrich	SKU: 89510
Carrier single-stranded DNA (ssDNA) from salmon testes	Sigma-Aldrich	SKU: D7656
Phosphate Buffer Saline (PBS)	ThermoFisher	Cat#10010023
Zymolyase	Zymo Research	Cat#E1006
Bathophenanthrolinedisulfonic acid disodium salt hydrate	Sigma-Aldrich	SKU: B1375
Cycloheximide	Research Products international	SKU: C81040–5.0
10x TBS	ThermoFisher	Cat#J62938.K7
Tween 20	Research Products International	SKU: P20370
HEPES (1M)	ThermoFisher	Cat#15630130
KCl	Research Products international	SKU: P41000–500.0; CAS: 7447-40-7
EDTA (0.5 M), pH 8.0	ThermoFisher	Cat#AM9261
Glass beads	Sigma-Aldrich	SKU: G8772
Pierce BCA Protein Assay Kits	ThermoFisher	Cat#23227
NuPAGE 10%, Bis-Tris Protein gels	ThermoFisher	Cat#NP0301

(Continued on next page)

Continued

REAGENT or RESOURCE	SOURCE	IDENTIFIER
MES buffer	ThermoFisher	Cat#NP0060
PVDF Transfer Membranes, 0.45 μm	ThermoFisher	Cat#88518
10x Tris Glycine buffer	BioRad	Cat#1610732
Methanol	ThermoFisher	Cat#268280025
Pierce ECL Western Blotting Substrate	ThermoFisher	Cat# 32106
Tris-HCl Buffer, 1M, pH7.5	ThermoFisher	Cat#15567027
MgCl ₂ , 2M	Sigma-Aldrich	SKU:68475-100ML-F
DTT, 1M	ThermoFisher	Cat#P2325
NAD ⁺ , 50mM	New England Biolabs	CatB9007S
Polyethylene glycol 8,000 (PEG-8000)	ThermoFisher	Cat#043443.36
Taq DNA Ligase	New England Biolabs	Cat#M0208S
T5 exonuclease	New England Biolabs	Cat#M0663S
Bsal-HFv2	New England Biolabs	Cat#R3733S

Deposited data

Raw reads and processed sequencing data	This paper	GEO: GSE193025
---	------------	----------------

Experimental models: Organisms/strains

W303a (HTLU-2832-1B: <i>HIS3</i> , <i>TRP1</i> , <i>LEU2</i> , <i>URA3</i> , <i>ADE2</i> , <i>can1</i>)	(Romero et al., 2019) ⁸	HB049
<i>cth1Δcth2Δ</i> (W303a <i>cth1Δ::hphB</i> , <i>cth2Δ::KanMX</i>)	This study	HB050
<i>SED1-3'UTR-3xHA</i> (<i>MATa his3Δ1 leu2Δ0 met15Δ0 ura3Δ0 SED1-3'UTR-3xHA-HIS3MX6</i>)	(Young et al., 2015) ¹⁶	HB085
<i>CWP2-3'UTR-3xHA</i> (<i>MATa his3Δ1 leu2Δ0 met15Δ0 ura3Δ0 CWP2-3'UTR-3xHA-HIS3MX6</i>)	(Young et al., 2015) ¹⁶	HB086
<i>CWP2-3'UTR-3xHA cth1Δcth2Δ</i> (<i>MATa his3Δ1 leu2Δ0 met15Δ0 ura3Δ0 CWP2-3'UTR-3xHA-HIS3MX6 cth1Δ cth2Δ::natMX</i>)	This study	HB107
<i>Mrs3-3xHA</i> (W303a <i>MRS3::MRS3-3xHA</i>)	This study	HB113
<i>Dph1-3xHA</i> (W303a <i>DPH1::DPH1-3xHA</i>)	This study	HB118
<i>Img1-3xHA</i> (<i>IMG1::IMG1-3xHA MRPS17::MRPS17-3xFLAG HAP1 MIP1(S) G1981A MATa</i>)	(Couvillion et al., 2016) ²⁷	HB056
<i>Img1-3xHA cth2Δ</i> (<i>IMG1::IMG1-3xHA cth2Δ MRPS17::MRPS17-3xFLAG HAP1 MIP1(S) G1981A MATa</i>)	This study	HB109
<i>Mrps17-3xHA</i> (<i>MRPS17::MRPS17-3xHA</i>)	(Couvillion et al., 2016) ²⁷	HB060
<i>Mrps17-3xHA cth2Δ</i> (<i>MRPS17::MRPS17-3xHA cth2Δ</i>)	This study	HB112

Oligonucleotides

MRS3-F	Azenta Life Sciences	AGGTTTGGCAGCATTTTATT
MRS3-R	Azenta Life Sciences	CCACACAGACAATGTATGAG
MRS3-AS-F	Azenta Life Sciences	CATACCCATAATGTTGCAC
MRS3-AS-R	Azenta Life Sciences	CCAAGAAATGCAATAAGTGC
DPH1-F	Azenta Life Sciences	GGGGTGTACTTCTGAAAGAT
DPH1-R	Azenta Life Sciences	CTCTGCTCTAACTCCACGA
DPH1-AS-F	Azenta Life Sciences	CTTCTTTCTCGATGAGAAA
DPH1-AS-R	Azenta Life Sciences	TTAAACGTTTTTGACGGCTT
MRS3-HA-F	Azenta Life Sciences	CTATATCATGGACAGCTTATGAATGTG CAAAACATTTCTAATGACGTATagcttag gtggaatgtacc

(Continued on next page)

Continued

REAGENT or RESOURCE	SOURCE	IDENTIFIER
MRS3-HA-R	Azenta Life Sciences	TCTGAGATGCAAAATGAAT GGAAAATAATATGACATGT AAGAATCAACTAgagttgactgagcagcgt
MRS3-HA-gRNA	Azenta Life Sciences	TTTCGAATAAACACACATAAACAAACA AAAGGAAACTGATGAGTCCG TGAGGACGAAACGAGTAAGCTCGTC TTTCCTAATGACGTATTAGTGTTTTAGAGC TAGAAATAGCAAGTAAAAATAAGGCTAG TCCGTTATCAACTTGAAAAAG TGGCACCGAGTCGGTGCTTTTGCCGGCA TGGTCCCAGCCTCCTCGCTGGCGCCGGC TGGGCAACATGCTTCGGCATGGCGA ATGGGACACAGGCCCTTT TCCTTTGTCGATA
DPH1-HA-F	Azenta Life Sciences	ATGGATTATTACGAAGCTAAAG GATACGGGCGTGGGGAAACTCAGAAACAT GCGATTGAAgacttagtggaatgacc
DPH1-HA-R	Azenta Life Sciences	TACTAACTATTTATACATATGTAA CAGGAAGACAAGTGACAACAAAACTATT TAAACTAgagttgactgagcagcgt
DPH1-HA-gRNA	Azenta Life Sciences	TTTCGAATAAACACACATAAACAAACAAAA TAGTTCTGATGAGTCCG TGAGGACGAAACGAGTAAGCTCGTCAAC TATCAATCGCATGTTTGTTTTAGAGC TAGAAATAGCAAGTAAAAATAAGGCTAG TCCGTTATCAACTTGAAAAAG TGGCACCGAGTCGGTGCTTTTGCCGGCA TGGTCCCAGCCTCCTCGCTGGCGCCGGC TGGGCAACATGCTTCGGCA TGGCGAATGGGACACAGGC CCCTTTTCTTTGTCGATA
cth1-deletion-gRNA	Azenta Life Sciences	TTTCGAATAAACACACA TAAACAAACAAAAATTCCTGATGAGTCCG TGAGGACGAAACGAGTAAGCTCGTCGAA TTTACAAAACTATCTCGTTTTAGAGC TAGAAATAGCAAGTAAAAATAAGGCTAG TCCGTTATCAACTTGAAAAAG TGGCACCGAGTCGGTGCTTTTGCCGGCA TGGTCCCAGCCTCCTCGCTGGCGCCGGC TGGGCAACATGCTTCGGCATGGCGAAT GGGACACAGGCCCTTTTCTTTGTCGATA
cth1-deletion-F	Azenta Life Sciences	TTCTCTCACGCTCTTGATCAGTGTGAGCAG TTACTAATATACTGGATCA GTCGGTCAACAACAAAGCCCTTTG AATATTTGGCGTATTTCTGCTGCCTCT
cth1-deletion-R	Azenta Life Sciences	AGAGGCAGCAGAAATACGCCAAATA TTCAAAGGGCTTTGTTGTTGAC CGACTGATCCAGTATATTAGT AACTGCTCACACTGATCAAG AGCGTGAGAGAA

(Continued on next page)

Continued

REAGENT or RESOURCE	SOURCE	IDENTIFIER
cth2-deletion-gRNA	Azenta Life Sciences	TTTCGAATAAACACACA TAAACAAACAAGAAGCACTGATGAG TCCGTGAGGACGAAACGAGTAAGCTCGTC TGCTTCTTTTCATCAGAGAGTTTAGAGC TAGAAATAGCAAGTTAAAATAAGGCTAG TCCGTTATCAACTGAAAAAG TGGCACCGAGTCGGTGCTTTTGGCCGGCA TGGTCCCAGCCTCCTCGCTGGCCGGCC TGGGCAACATGCTTCGGCATGGC GAATGGGACACAGGCCCTTTTC CTTTGTGCGATA
cth2-deletion-F	Azenta Life Sciences	AGAGAAAAGCGAAACAGTGCTGCAAAC TCAATACGTAATAAATAACGCAAT AACAAATCCTGGCCTGGCGAAGACC GGCGTCTCAACTAACTCAATTATT
cth2-deletion-R	Azenta Life Sciences	AATAATTGAGTTTAGTTGAGACGCCGGTC TTCGCCAGGCCAGGAATTGTT ATTGGTTATTTTTACGTATTG AGTTTGACAGCACTGTTTCGCTTTCTCT
CTH2:natMX-F	Azenta Life Sciences	AAACAGTGCTGCAAACCAATACG TAAAAATAACGCAATATGTGGGC TCGATCTGTTAGCTTGCCCTCG
CTH2:natMX-R	Azenta Life Sciences	TTTAGTTGAGACGCCGGTCTTCGCCAGGC CAGGAATTGTTTGTGGATCTGA TATCATCGATG
MRS3-AS-ORF-F	Azenta Life Sciences	GGactagtATGGTAGAAAACCTCGTCGAGTAA
MRS3-AS-ORF-R	Azenta Life Sciences	TTgcgccgcCTAATACGTC TTAGGAAATGTT
MRS3-AS-1-300-R	Azenta Life Sciences	TTgcgccgcACCTAGTATGACAG ACTGAACAC
MRS3-AS-1-600-R	Azenta Life Sciences	TTgcgccg cATTAATGCTGCAAATGGGATGT
MRS3-AS-601-945-F	Azenta Life Sciences	GGactagtTTCGTCATATATGAATCATCCAC
CBP3-qPCR F	Azenta Life Sciences	GGGGTGAAGGTCGAAAAACT
CBP3-qPCR R	Azenta Life Sciences	AGCCTACTTCTCTCGCTTGG
CBP4-qPCR F	Azenta Life Sciences	CATTGTGGGTACGTTGGTTG
CBP4-qPCR R	Azenta Life Sciences	TTGATCTGTTGGCGTTGTGT
CBP6-qPCR F	Azenta Life Sciences	AACAGAACTTCCGGTCCATT
CBP6-qPCR R	Azenta Life Sciences	GCTCGTTGATGCTTTCTTCC
MRPL36-qPCR F	Azenta Life Sciences	TGGAGTTGAGTGATGGAAGT
MRPL36-qPCR R	Azenta Life Sciences	GCGGATTATTTCTCTGGTCTTG
MRPL32-qPCR F	Azenta Life Sciences	GGAAAACGCATACCGCTAAA
MRPL32-qPCR R	Azenta Life Sciences	CCAGGATATAGGACTCTTTGGTCT
MRPL25-qPCR F	Azenta Life Sciences	TGCCCAAGGGTCATAAGCA
MRPL25-qPCR R	Azenta Life Sciences	GGAAGCAATCAACTCATCTACC
TOM20-qPCR F	Azenta Life Sciences	TGTCCCAGTCGAACCCTATC
TOM20-qPCR R	Azenta Life Sciences	TGCGGGCTATTTCTTCTTTG
HSP60-qPCR F	Azenta Life Sciences	TCCAATCAAAGCAGAAGACC
HSP60-qPCR R	Azenta Life Sciences	CAAAATACAAGCCGCAAGAG

(Continued on next page)

Continued

REAGENT or RESOURCE	SOURCE	IDENTIFIER
BCS1-qPCR F	Azenta Life Sciences	ACTCCGCCAACAAATGAAAC
BCS1-qPCR R	Azenta Life Sciences	TGACATAGCATCGCCAACT
Recombinant DNA		
Plasmid: pCEV-MRS3 ^{Δ5}	This study	pVL067
Plasmid: pCEV-MRS3-AS ¹⁻³⁰⁰	This study	pVL068
Plasmid: pCEV-MRS3-AS ¹⁻⁶⁰⁰	This study	pVL069
Plasmid: pCEV-MRS3-AS ⁶⁰¹⁻⁹⁴⁵	This study	pVL070
Plasmid: pCEV-MRS3-AS ³⁰¹⁻⁹⁴⁵	This study	pVL071
Plasmid: pCEV-MRS3-AS ³⁰¹⁻⁶⁰⁰	This study	pVL072
Software and algorithms		
STAR 2.7.1a	(Dobin et al., 2013) ³³	https://www.encodeproject.org/software/star/
Rsubread 1.22.2	(Liao et al., 2019) ³⁴	https://www.rdocumentation.org/packages/Rsubread/versions/1.22.2
Prism 9.3.1	GraphPad	https://www.graphpad.com/scientific-software/prism/
EdgeR	(Robinson et al., 2010) ³⁵	https://bioconductor.org/packages/release/bioc/html/edgeR.html
Limma	(Ritchie et al., 2015) ³⁶	https://bioconductor.org/packages/release/bioc/html/limma.html
Other		
NanoDrop 2000 Spectrophotometer	ThermoFisher	ND-2000
Epoch2 Microplate Spectrophotometer	BioTek	EPOCH2TC

RESOURCE AVAILABILITY

Lead contact

Further information and requests for resources and reagents should be directed to and will be fulfilled by the Lead Contact, Vyacheslav M. Labunsky (vlabuns@bu.edu).

Materials availability

The east strains and plasmids generated by this study are listed in the [key resources table](#) and are available from the [lead contact](#) without restriction.

Data and code availability

- RNA-Seq and Ribo-Seq data generated in this study are available at NCBI GEO under the accession number GSE193025 (<https://www.ncbi.nlm.nih.gov/geo/query/acc.cgi?acc=GSE193025>).
- This study did not generate new code.
- Any additional information required to reanalyze the data reported in this paper is available from the [lead contact](#) upon request.

EXPERIMENTAL MODEL AND STUDY PARTICIPANT DETAILS

Yeast strains

The yeast strains used in this study and their genotypes are listed in [key resources table](#). One-step polymerase chain reaction (PCR)-mediated gene disruption was performed using standard techniques to delete genes of interest. The genotypes of the resulting strains were verified using colony PCR. Prototroph W303a (*MATa*, *HIS3*, *TRP1*, *LEU2*, *URA3*, *ADE2*, *can1*) and W303a *cth1Δcth2Δ* (*cth1Δ::hphB*, *cth2Δ::KanMX*) cells were cultured at 30°C in liquid SD medium (0.17% yeast nitrogen base without ammonium sulfate and without amino acids, 2% D-glucose, and 2 g/L Kaiser drop-out (Formedium)). For induction of Fe deficiency, cells were initially grown to OD₆₀₀ = 0.2 and Fe²⁺ chelator bathophenanthrolinedisulfonic acid (BPS) was added to the final concentration 100 μM. Following the addition of BPS, cells were incubated for 3 h and 6 h. Cells were collected by rapid filtration through 0.45 μm membrane filters using a glass holder filter assembly, scrapped with a

spatula, and flash frozen in liquid nitrogen. Yeast strains encoding HA-tagged Mrs3 and Dph1 proteins were generated using CRISPR/Cas9 genome editing.³⁷

METHOD DETAILS

Ribo-Seq and RNA-seq sequencing, data processing, and analysis

Yeast extracts were prepared by cryogrinding the cell paste with BioSpec cryomill. The cell paste was re-suspended in lysis buffer (20 mM Tris-HCl pH 8, 140 mM KCl, 5 mM MgCl₂, 0.5 mM DTT, 1% Triton X-100, 100 µg/mL cycloheximide), spun at 20,000 × g at 4°C for 5 min and 1 mL of the supernatant was divided into two tubes, for total mRNAs and footprint extraction. For Ribo-Seq, 50 OD₂₆₀ units of the lysate (in 1 mL of lysis buffer) were treated with 10 µL of RNase I (100 U/µL) for 1 h, with gentle rotation of samples at room temperature. Then, 1 mL of RNase-treated lysate was layered on a sucrose gradient for isolation of monosomes using ultracentrifugation followed by footprint extraction with hot acid phenol method. For RNA-Seq samples, poly(A) mRNA isolation was performed using a poly(A) mRNA isolation kit with subsequent mRNA fragmentation. The RNA-seq and Ribo-Seq libraries were prepared using the ARTseq Ribosome Profiling kit (Illumina)³⁸ and sequenced using the Illumina HiSeq platform.

For Ribo-Seq data, the adapter sequence was removed using Cutadapt 4.1³⁹ and reads less than 23 nucleotides were filtered out. The Ribo-Seq and RNA-Seq reads were aligned to the *S. cerevisiae* genome from the Saccharomyces Genome Database (<https://www.yeastgenome.org/>, release number R64-2-1). Sequence alignment was performed using STAR software 2.7.1a, allowing two mismatches per read.³³ Counts were generated with featureCounts from Rsubread 1.22.2 package.³⁴ We filtered out genes with low number of reads (less than 10 counts in less than 66.6% of samples) resulting in 5506 detected genes in RNA-Seq and 5069 genes in Ribo-Seq expression matrices. Identification of differentially expressed genes was performed using the generalized linear model of the EdgeR package (GLM, glmFit, glmLRT) with an adjusted *p*-value cutoff (FDR<0.05).³⁵

Ribosome occupancy analysis

To estimate translational efficiency changes during Fe deficiency, we analyzed ribosomal occupancy (RO), which represents a ratio between ribosomal footprints and mRNA abundance allowing to identify actively translated transcripts. To calculate RO, genes with low counts (less than 10 counts) were filtered out from RNA-Seq and Ribo-Seq datasets containing raw counts. RNA-Seq and Ribo-Seq data were then RLE normalized ("Relative Log Expression" normalization) using the edgeR package³⁵ and RO was calculated using the following formula: $\log_2(\text{Ribo-seq counts} + 1) - \log_2(\text{RNA-seq counts} + 1)$. We used Limma R package to estimate the **contribution of transcriptional and translational regulation to gene expression changes** and identify translationally regulated genes.^{36,40}

Quantification of antisense transcripts

To quantify antisense transcripts, sequence reads that align to annotated ORFs and are transcribed from the opposite DNA strand were counted using featureCounts from Rsubread 1.22.2 package.³⁴ First, we filtered out genes with less than 5 counts in less than 66.6% of samples (an empirically chosen threshold aiming to bring the distribution of the counts closer to normal and preserve the maximum number of genes with minimal variation between replicates). After filtering step, we obtained 726 genes. RLE normalized counts were then used to identify differentially expressed antisense transcripts during Fe deficiency using Limma R package.

Polysome analysis

Polysome analysis was performed according to the previously published protocol.¹¹ Cells were grown in SC media overnight upon 0.2 OD₆₀₀ density and supplemented with 100 µM of the bathophenanthroline disulfonate (BPS) to induce Fe deficiency. After 3 and 6 h, cells were treated with 50 µg/mL cycloheximide (CHX) for 5 min and, after lysis, collected and resuspended in 700 µL of lysis buffer [20 mM Tris-HCl, pH 8, 140 mM KCl, 5 mM MgCl₂, 0.5 mM dithiothreitol, 1% Triton X-100, 0.1 mg/mL CHX, and 0.5 mg/mL heparin]. Aliquots of cell extracts containing 8.5 OD₂₆₀ units were loaded on top of sucrose gradients (5–50% w/w). The gradients were sedimented at 35,000 rpm at 4°C in an SW41 rotor (Beckman) for 2 h 40 min. Fractions were analyzed by UV detection at 260 nm.

RT-qPCR

Total RNA was isolated by hot acid phenol extraction. RNA was treated with DNaseI, and 1 µg of RNA was used for cDNA synthesis using SuperScript III reverse transcriptase (Thermo Fisher Scientific) with random hexamer primers according to manufacturer's instructions. mRNA expression was then analyzed by real-time PCR using KAPA SYBR FAST qPCR Master Mix (Kapa Biosystems) and the CFX-96 Touch Real-Time PCR Detection System (Bio-Rad Laboratories). *ACT1* was used as a reference gene for normalization of mRNA expression between genotypes. The primers used for RT-qPCR are listed in [key resources table](#). Results are represented as means ± SEM from three independent experiments.

Western blot analysis

Total protein extracts were prepared using TCA precipitation. 5 OD₆₀₀ units of cells were resuspended in 0.5 mL of 6% TCA, incubated at least 10 min on ice and centrifuged for 5 min at 4°C at maximum speed (~14,000 × g). Next, the pellet was washed twice with acetone and air-dried. The pellet was then resuspended in 250 µL of HU buffer (5 M urea, 50 mM Tris-HCl pH 7.5, 1% SDS, 1 mM PMSF) and samples were

homogenized with glass beads by vortexing at maximum speed for 10 × 30 s. Equal amounts of proteins were resolved in 10% SDS-PAGE gels and transferred to PVDF membrane. Anti-HA-Peroxidase, High Affinity (3F10) rat monoclonal antibody (Roche) was used to detect HA-tagged proteins. Mouse anti-Pgk1 monoclonal antibody (Life Technologies) and HRP-conjugated secondary anti-mouse antibody (Santa Cruz Biotechnology) were used to detect Pgk1 protein levels as a loading control. Original full size Western blot images are provided in [Figures S9](#) and [S10](#).

Expression of the *MRS3^{AS}* lncRNA

To generate plasmids that express the *MRS3^{AS}* lncRNA, the sequence containing *MRS3* ORF (or indicated fragments) was PCR amplified from yeast genomic DNA and integrated in reverse orientation under the control of *TEF1* promoter into pCEV plasmid⁴¹ using *SpeI* and *NotI* restriction sites. *W303a* yeast cells were transformed with pCEV-*MRS3^{AS}* plasmids and selected on media containing Zeocin at a final concentration of 300 μg/mL. Expression of the antisense *MRS3^{AS}* transcript was verified using RT-qPCR.

Heme quantification

For induction of Fe deficiency, cells were initially grown to $OD_{600} = 0.2$ and Fe^{2+} chelator bathophenanthrolinedisulfonic acid (BPS) was added to the final concentration 100 μM. Following the addition of BPS, cells were incubated for 3 h and 6 h. Intracellular heme levels were assessed using the oxalic acid method. Briefly, overnight yeast cultures were diluted to $OD_{600} = 0.2$ units/mL and grown until cells reached $OD_{600} = 0.8$ units/mL. Subsequently, 8 OD_{600} units of cells were harvested by centrifugation at 2,500 × g, washed with distilled water, and the pellet was resuspended in 500 μL of 20 mM oxalic acid. An additional 500 μL of 2 M oxalic acid was added, and the suspension was divided equally into two tubes. One set of sample tubes was placed in a heating block at 100°C for 45 min, while the other set of samples was kept at room temperature for the same duration as a baseline. Following incubation, samples were cooled to room temperature, and 100 μL of suspension was transferred per well into a black-well 96-well plate in duplicates. The fluorescence of porphyrin was measured using a Biotek plate reader with 400 nm excitation and 662 nm emission. Baseline values (from parallel unheated samples in oxalic acid) were subtracted, and the relative fluorescence intensity in arbitrary units (A.F.U.) was plotted.

QUANTIFICATION AND STATISTICAL ANALYSIS

Statistical analysis was performed using Prism 9.3.1 (GraphPad Software, Inc). Statistical significance of the RT-qPCR data was determined by calculating *p* values using one-way ANOVA. Error bars represent standard errors of the means (SEM). The information about number of replicates and *p* values can be found in figure legends. For RNA-Seq and Ribo-Seq analyses, three biological replicates were analyzed per each condition.